Atmospheric
Measurement
Techniques

Open Access

Droplet activation of wet particles: development of the Wet CCN approach

S. Nakao[1], S. R. Suda[2], M. Camp[3], M. D. Petters[2], and S. M. Kreidenweis[1]

[1]Department of Atmospheric Science, Colorado State University, Fort Collins, CO, USA
[2]Department of Marine, Earth, & Atmospheric Sciences, North Carolina State University, Raleigh, NC, USA
[3]Department of Civil and Environmental Engineering, Rice University, Houston, TX, USA

Correspondence to: S. Nakao (shunsuke1027@gmail.com)

Abstract. Relationships between critical supersaturation required for activation and particle dry diameter have been the primary means for experimentally characterizing cloud condensation nuclei (CCN) activity; however, use of the dry diameter inherently limits the application to cases where the dry diameter can be used to accurately estimate solute volume. This study challenges the requirement and proposes a new experimental approach, Wet CCN, for studying CCN activity without the need for a drying step. The new approach directly measures the subsaturated portion of the Köhler curves. The experimental setup consists of a humidity-controlled differential mobility analyzer and a CCN counter; wet diameter equilibrated at known relative humidity is used to characterize CCN activity instead of the dry diameter. The experimental approach was validated against ammonium sulfate, glucose, and nonspherical ammonium oxalate monohydrate. Further, the approach was applied to a mixture of nonspherical iodine oxide particles. The Wet CCN approach successfully determined the hygroscopicity of nonspherical particles by collapsing them into spherical, deliquesced droplets. We further show that the Wet CCN approach offers unique insights into the physical and chemical impacts of the aqueous phase on CCN activity; a potential application is to investigate the impact of evaporation/co-condensation of water-soluble semivolatile species on CCN activity.

1 Introduction

In addition to their key roles in the prediction of climate changes (IPCC, 2007), clouds are also important drivers of atmospheric chemistry, impacting aerosol formation, modification, and removal (Graedel and Weschler, 1981; Blando and Turpin, 2000; Ervens et al., 2011). One aspect of clouds that is presently not well understood is the beginning of their lifetime: cloud droplet activation. The aerosol particles that serve as nuclei for cloud droplets are called cloud condensation nuclei (CCN). The number concentration of available CCN influences cloud droplet size, and thereby reflectivity (Twomey, 1974), as well as cloud lifetime (Albrecht, 1989). Accurate description of the cloud droplet activation process continues to be an active research area (McFiggans et al., 2006; Andreae and Rosenfeld, 2008; Ruehl et al., 2012; Sareen et al., 2013; Topping et al., 2013).

The equilibrium between water vapor and a water-containing atmospheric aerosol particle depends on the particle (or droplet) size and its physicochemical parameters, i.e., moles of dissolved molecules (or dissociated ions), solution non-ideality, and surface tension (Pruppacher and Klett, 1997; Seinfeld and Pandis, 2006); for solid particles that take up water via an adsorption process, surface properties are important (Sorjamaa and Laaksonen, 2007; Kumar et al., 2009, 2011). Early research on CCN recognized the major contribution of inorganic salts, primarily ammonium sulfate, to the composition of CCN (Twomey, 1971). Currently organic compounds are also recognized as important constituents of CCN due to their abundance and water solubility (Novakov and Penner, 1993). However, the chemical composition of organic-containing CCN remains largely unknown since aerosol-phase organics comprise numerous compounds and only around 10–30 % of these can be identified by current analytical techniques (Hallquist et al., 2009).

Since physicochemical parameters are mostly unknown for atmospheric organic aerosol-phase species, a number of simple and computationally inexpensive parameterization

approaches have been developed for the prediction of CCN activity (Fitzgerald et al., 1982; Hudson and Da, 1996; Rissler et al., 2006; Petters and Kreidenweis, 2007; Wex et al., 2007). Although each parameterization approach differs slightly in its treatment of physicochemical properties of solutes, a common constraint of any of the previous parameterizations is the requirement that the available volume of solute is specified. Experimentally, this solute volume has been determined by measurement of the dry particle mobility diameter. However, previous studies reported observational artifacts arising from the drying of aerosols, such as residual water remaining in the dried particles and being erroneously assumed to contribute to the volume of solute; hydrate formation, also leading to overestimates of dry solute mass; and evaporative loss of some aerosol components (e.g., Prenni et al., 2001; Hori et al., 2003; Mikhailov et al., 2004). An additional complication is that dry nonspherical particles may collapse when exposed to high humidity (e.g., Martin et al., 2013), so that the volume change upon wetting cannot be used to deduce the amount of water added to the particle.

To address these challenges, this study developed a new experimental approach, "Wet CCN", to characterize hygroscopicity without the need for accurate characterization of the particle dry diameter. Proof-of-concept experiments were carried out with lab standards as well as for iodine oxide particles (IOP). Previous studies observed that IOP contributed to new particle formation in coastal areas; however, there has been debate over its chemical identity as inferred from hygroscopicity measurements (Jimenez et al., 2003; McFiggans et al., 2004; Murray et al., 2012; Saiz-Lopez et al., 2012). IOP was reported to have characteristics that are particularly well-suited for testing the utility of the Wet CCN approach: nucleated particles are nonspherical; there is the potential for the formation of hydrates ($I_2O_5 \cdot H_2O$); and IOP appears to retain water when dried. Based on the findings from these proof-of-concept studies, the limitations and potential applications of the new approach were assessed.

2 Theoretical development: Köhler theory without dry diameter

Köhler theory predicts saturation ratio S over an aqueous droplet (Pruppacher and Klett, 1997). A widely used form of Köhler theory is the following (e.g., Kreidenweis et al., 2005):

$$S(D) = a_w \exp\left(\frac{A}{D}\right),$$

$$A = \frac{4\sigma_{s/a}(T) M_w}{RT\rho_w}, \tag{1}$$

where a_w is the activity of water in solution, $\sigma_{s/a}$ is the temperature-dependent surface tension of the solution–air interface (Christensen and Petters, 2012), M_w is the molecular weight of water, R is the universal gas constant, T is the

temperature, ρ_w is the density of water, and D is the diameter of the droplet. S is equivalent to the relative humidity, RH, expressed as a fraction. One of the common ways to express the water activity–particle composition relationships is (Kreidenweis et al., 2005; Rose et al., 2008; Kreidenweis et al., 2009)

$$a_w^{-1} = 1 + \nu\Phi \frac{n_s}{n_w} = 1 + \nu\Phi \frac{\rho_s M_w}{\rho_w M_s} \frac{V_s}{V_w}, \tag{2}$$

where ν is the stoichiometric dissociation number for the solute (e.g., $\nu_{NaCl} = 2$), Φ is the molal or practical osmotic coefficient that accounts for solution non-idealities, n_s is the moles of solute, n_w is the moles of water, ρ_s is the density of the solute, M_s is the molecular weight of solute, V_s is the volume of dry solute, and V_w is the volume of water.

From Eqs. (1) and (2), an expression for the critical saturation ratio (S_c), the maximum S of the Köhler curve (Eq. 1) for a given particle composition, can be derived as follows (Seinfeld and Pandis, 2006; Kreidenweis et al., 2009):

$$\ln(S_c) \approx \left(\frac{4A^3}{27B^3}\right)^{1/2}, \tag{3}$$

$$B = \nu\Phi \frac{\rho_s M_w}{\rho_w M_s} D_{dry}^3,$$

where D_{dry} is the dry diameter, A relates to the Kelvin effect (Eq. 1), and B relates to the solute effect. It is also customary to define critical supersaturation (s_c), where $s_c = S_c - 1$. The approximation in Eq. (3) applies to a dilute solution, which is typically a reasonable assumption for cloud droplet activation. To further simplify the examination of the role of particle chemical composition in Köhler theory, Petters and Kreidenweis (2007) proposed an alternative form of Eq. (2), introducing a single hygroscopicity parameter, κ, as an intrinsic property of a particle with specified chemical composition:

$$a_w^{-1} = 1 + \kappa \frac{V_s}{V_w}, \tag{4}$$

$$\kappa = \nu\Phi \frac{\rho_s M_w}{\rho_w M_s} = \frac{B}{D_{dry}^3}.$$

For an ideal solution ($\Phi = 1$), Raoult's law leads to κ_{Raoult} (Petters et al., 2009b)

$$\kappa_{Raoult} = \nu \frac{\rho_s M_w}{\rho_w M_s}. \tag{5}$$

From Eqs. (1), (3), and (4) (Petters and Kreidenweis, 2007)

$$S = \frac{D^3 - D_{dry}^3}{D^3 - D_{dry}^3(1-\kappa)} \exp\left(\frac{A}{D}\right), \tag{6}$$

$$\ln(S_c) \approx \left(\frac{4A^3}{27\kappa D_{dry}^3}\right)^{\frac{1}{2}}. \tag{7}$$

Note that Eq. (7) is valid for $\kappa > 0.2$, but may be used for $\kappa > \sim 0.01$ if small numerical errors are acceptable (Petters and Kreidenweis, 2013).

This study aims to determine κ without the need for accurate characterization of D_{dry}. Our approach is to eliminate D_{dry} and use S and D as alternative constraints. By solving Eq. (7) for D_{dry} and substituting to Eq. (6),

$$S = \frac{D^3 - \frac{4A^3}{27\kappa\ln^2(S_{\text{c}})}}{D^3 - \frac{4A^3}{27\kappa\ln^2(S_{\text{c}})}(1-\kappa)} \exp\left(\frac{A}{D}\right). \qquad (8)$$

Equation (8) shows that κ can be determined from simultaneous measurements of S, D, S_{c}, and A. In this study, A is computed for surface tension of water ($\sigma_{\text{s/a}} = 0.072\,\text{J m}^{-2}$) and $T = 298.15\,\text{K}$. The experimental section below describes how to determine S, D, and S_{c}.

An alternative approach to eliminating D_{dry} is to start from the definition of κ (Eq. 4). Particle hygroscopic growth can be calculated by rearranging Eq. (4) as follows:

$$D = D_{\text{dry}}\left(1 + \kappa\frac{a_{\text{w}}}{1-a_{\text{w}}}\right)^{1/3}, \qquad (9)$$

or converting a_{w} to S (Eq. 1),

$$D = D_{\text{dry}}\left(1 + \kappa\frac{S/\exp\left(\frac{A}{D}\right)}{1 - S/\exp\left(\frac{A}{D}\right)}\right)^{1/3}. \qquad (10)$$
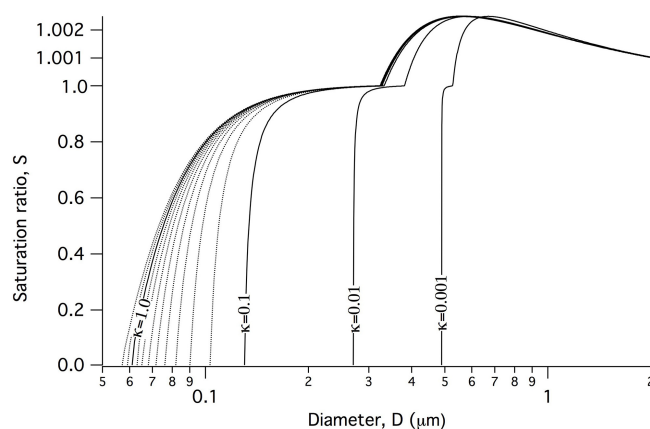
Again, D_{dry} can be eliminated using Eq. (7):

$$D = \left(\frac{4A^3}{27\kappa\ln^2(S_{\text{c}})}\right)^{1/3}\left(1 + \kappa\frac{S/\exp\left(\frac{A}{D}\right)}{1 - S/\exp\left(\frac{A}{D}\right)}\right)^{1/3}, \qquad (11)$$

which is merely a different form of Eq. (8). Equation (11) may provide a more intuitive interpretation; the first term in Eq. (11) is based on cloud droplet activation, and the second term is based on hygroscopic growth. Solutions of Eq. (8) (or Eq. 11) can be plotted as contours of S vs. D for a set of κ, for a chosen S_{c} (Fig. 1).

Snider et al. (2006) developed a similar technique, "the wet-selection technique", in which deliquesced inorganic particles, mobility selected at a prescribed S, are introduced into the Wyoming CCN instrument, in order to characterize the sphere-equivalent dry size (D_{se}) of nonspherical particles (e.g., NaCl) using Köhler theory. For pure compounds with well-understood physicochemical properties, their approach is essentially the same as ours. The advantage of our approach is its capability in studying particles with unknown chemical composition, enabled by the use of κ.

The implicit assumption in this approach that κ is constant throughout the entire range of S may not be valid in some cases. A number of studies investigated κ both at supersaturated conditions (κ_{CCN} determined by a CCN counter) and subsaturated conditions (κ_{gf} calculated from a growth factor
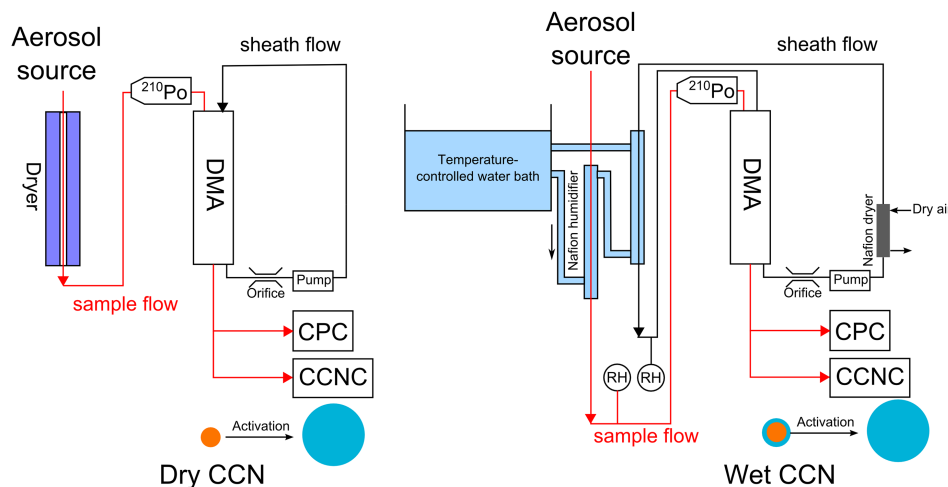

Figure 1. Calculated saturation ratios of water (S) as functions of (wet) diameter (D) for $0.001 < \kappa < 1.2$ compounds (s_{c}: 0.25 %).

determined by a hygroscopicity-tandem differential mobility analyzer, H-TDMA) (Prenni et al., 2007; Carrico et al., 2008; Duplissy et al., 2008; Petters et al., 2009a; Massoli et al., 2010; Alfarra et al., 2013; Jurányi et al., 2013; Martin et al., 2013; Wu et al., 2013; Hong et al., 2014), with different levels of agreement between κ_{CCN} and κ_{gf}. For instance, κ_{gf} of secondary organic aerosol (SOA) is often observed to be lower than κ_{CCN} (Prenni et al., 2007; Petters et al., 2009c; Wex et al., 2009; Massoli et al., 2010). Possible causes for the gap between κ_{CCN} and κ_{gf} include non-ideality and solubility of complex organic mixtures (Petters et al., 2009c). The impacts of this assumption ($\kappa_{\text{CCN}} = \kappa_{\text{gf}}$) and of experimental error on the derived values of κ are discussed in detail in the error analysis Sect. 3.3.

3 Experimental methods

3.1 Dry CCN and Wet CCN

The Wet CCN experimental setup is similar to that used for the Dry CCN approach described elsewhere (Petters et al., 2007), except that the aerosol sample is equilibrated to a known relative humidity prior to size selection (Fig. 2). The sample humidity was controlled in a similar way as in Suda and Petters (2013): the sample air was passed through Nafion tubes (PermaPure, MH-110, OD 0.27 cm, length 30.5 cm) with temperature-controlled water (Cole-Parmer, six-liter programmable digital controller refrigerated/heated circulating bath, EW-12118-30) circulating in the annular region. The residence time between the humidifier and the differential mobility analyzer (DMA) is ~ 6 s, which is enough time for particles to equilibrate to the new S such that the measured size D reflects the measured S (Snider and Petters, 2008; Suda and Petters, 2013). Both the aerosol sample flow and the sheath flow were humidified. The relative humidities in both flows were measured by humidity sensors

Figure 2. Experimental setup for Dry CCN and Wet CCN analyses.

(Rotronic, Hygroclip, HC2-S; ±0.8 % RH/±0.1 K accuracy at 23 ± 5 °C; valid at 10, 35, and 80 % RH; calibrated by RH Systems/MBW 97, s/n 06-0808). The humid aerosol flow was introduced into a chamber holding four ^{210}Po strips to equilibrate the aerosol charge distribution. A differential mobility analyzer (TSI 3071A) operating at 9 L min^{-1} sheath flow and 1.4 L min^{-1} monodisperse flow was used to select a quasi-monodisperse sample of humidified particles; the voltage was increased stepwise to select particles with mobility diameters ranging from 40 nm to 300 nm. The recirculating sheath flow of the DMA was slightly dried by flowing dry air through a Nafion tube (PermaPure, MH-110) before humidification in order to avoid condensation in the line. The monodisperse aerosol flow was split and sent to a condensation particle counter (CPC; TSI 3010) to record total particle number concentration and to a Droplet Measurement Technologies Cloud Condensation Nuclei Counter (DMT CCNC) (Roberts and Nenes, 2005), held at a fixed supersaturation, to record activated droplet number concentrations.
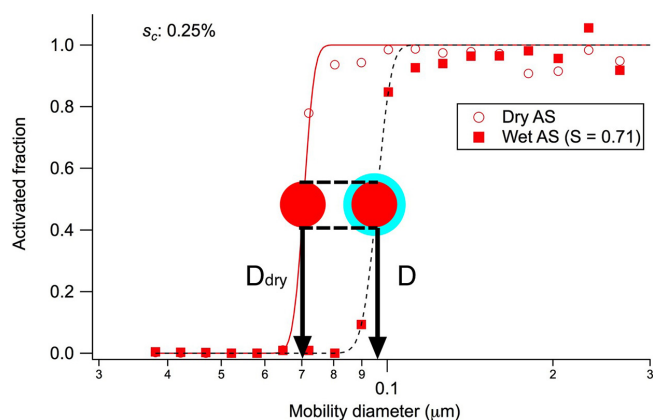
The calibration and analysis of activation curves for dry aerosol were described in detail by Petters et al. (2009a). The contributions from multiply charged particles to the activation curves were removed by an inversion matrix (Petters et al., 2009a). The activation curves were fitted to a cumulative Gaussian function and the diameter at which 50 % of the particles activated was used as D_{dry}. The supersaturation was calibrated against ammonium sulfate (Fisher Scientific, > 99 %, A702), based on Köhler theory (Eq. 1) and E-AIM (Wexler and Clegg, 2002), in which the mole fraction of water in ammonium sulfate solution was calculated for varied relative humidity (a_w for a bulk solution), and S_c was determined by searching for the maximum in S (accounting for the Kelvin effect) for the experimentally determined D_{dry}. For the range of S_c investigated in this study (1.0025–1.0040), κ as determined from E-AIM water activities ranges from 0.61 to 0.59.

Experiments were conducted using particles composed of glucose (Sigma-Aldrich, D-(+)-glucose, > 99.5, G8270), ammonium oxalate monohydrate (Sigma-Aldrich, > 99.5 %, 09898), ammonium nitrate (Fisher Scientific, > 98 %, A676), and iodine oxide particles (IOP) as described below. Ammonium sulfate, glucose, ammonium oxalate, and ammonium nitrate aerosols were generated from aqueous solutions using a TSI 3076 constant output atomizer.

Wet particle diameter D was measured in the same manner as D_{dry}, except that the particles were humidified and thus may have been wet. Example data for ammonium sulfate activation are shown in Fig. 3, where the activation curves (activated fraction vs. diameter) of dry and wet ammonium sulfate are compared. For a given critical supersaturation (s_c) set by the CCNC, the shift in activation curve in Fig. 3 is only due to the presence of water since the moles of solute needed for activation (n_s) are independent of the liquid water content of the initial aerosol. Note that when the sample is dry, $D50$ and D are equal to D_{dry}.

3.2 Generation of iodine oxide particles (IOP)

Experiments were carried out in a 65 L stainless steel tank operating as a batch reactor. The reactor was flushed with O_3 generated by an ozone generator (Teledyne Instruments, Model 703) to reach estimated initial O_3 concentrations of 1–2 ppm. CH_2I_2 (99 %, Sigma Aldrich, 158429) was injected into the reactor by doping 1 µL of 10 vol % solution of CH_2I_2 in methanol on glass wool in a manifold and gently flushing 3 L of warm air through the manifold (calculated concentration of CH_2I_2: 0.47 ppm). Due to the small size of the reactor, experiments were carried out at concentration ranges several orders of magnitude higher than previous chamber studies (Jimenez et al., 2003; CH_2I_2: 0.015–50 ppb; O_3: 100–500 ppb; 28 m^3 Caltech indoor chamber). Higher concentrations may impact aerosol composition by influencing
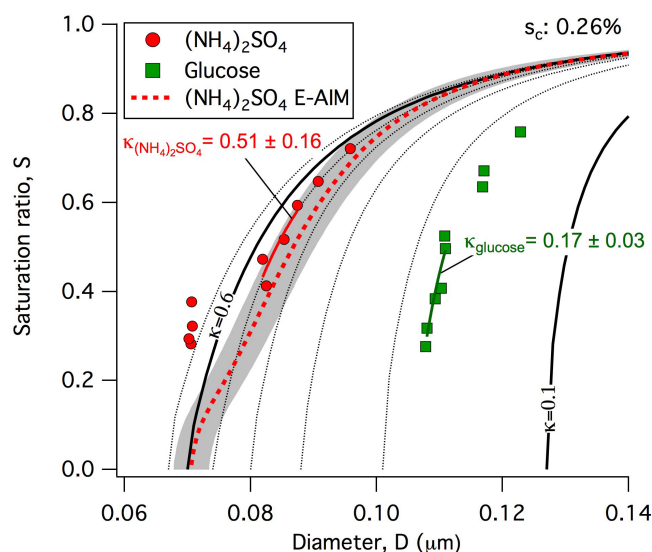
Figure 3. Example activation curves of dry and wet ammonium sulfate (AS) particles. At a given critical supersaturation (s_c), the moles of AS needed for activation at this supersaturation are fixed, irrespective of initial particle state. Therefore, the activation curve of wet AS is shifted toward larger particles size (D), compared to dry AS (D_{dry}). The shift corresponds to the water content of the humidified particle.

Figure 4. Data obtained using the Wet CCN method for ammonium sulfate and glucose particles. Theoretical prediction for $(NH_4)_2SO_4$ is made by calculating hygroscopic growth by E-AIM and assuming volume additivity for solute and water, with $\pm 4\%$ variation in terms of D (shaded area).

reaction kinetics and partitioning of higher volatility products to the condensed phase. Therefore caution must be taken in extrapolating the results to atmospheric conditions. The scope of the IOP experiments in this study is to evaluate the applicability of the Wet CCN approach to a previously studied system producing nonspherical particles with unknown composition. Jimenez et al. (2003) observed qualitatively different hygroscopicities of IOP formed in dry vs. humid conditions, with the humid reaction producing nonhygroscopic IOP and the dry reaction producing highly hygroscopic IOP, possibly due to differences in gas-phase chemistry.

3.3 Validation and error analysis

To develop estimates of the error associated with the proposed approach, the Wet CCN analysis of ammonium sulfate was tested against a model prediction (Fig. 4). The theoretical line for ammonium sulfate represents D_{dry} (x-intercepts), that is, the typical calibration measurement in the Dry CCN method used to determine s_c, as described above (Sect. 3.1), and subsequent hygroscopic growth taking into account the non-ideality of the solution using E-AIM (Wexler and Clegg, 2002). One can consider the S vs. D space analogous to humidograms, in which hygroscopic growth factors (GF = D/D_{dry}) are plotted against a_w (Carrico et al., 2008); the key advantage of the S vs. D space is that there is no explicit requirement to specify D_{dry}. Note that S vs. D can be reduced to the conventional humidogram by taking the diameter ratio (D/D_{dry}) and converting S to a_w (Eq. 1).
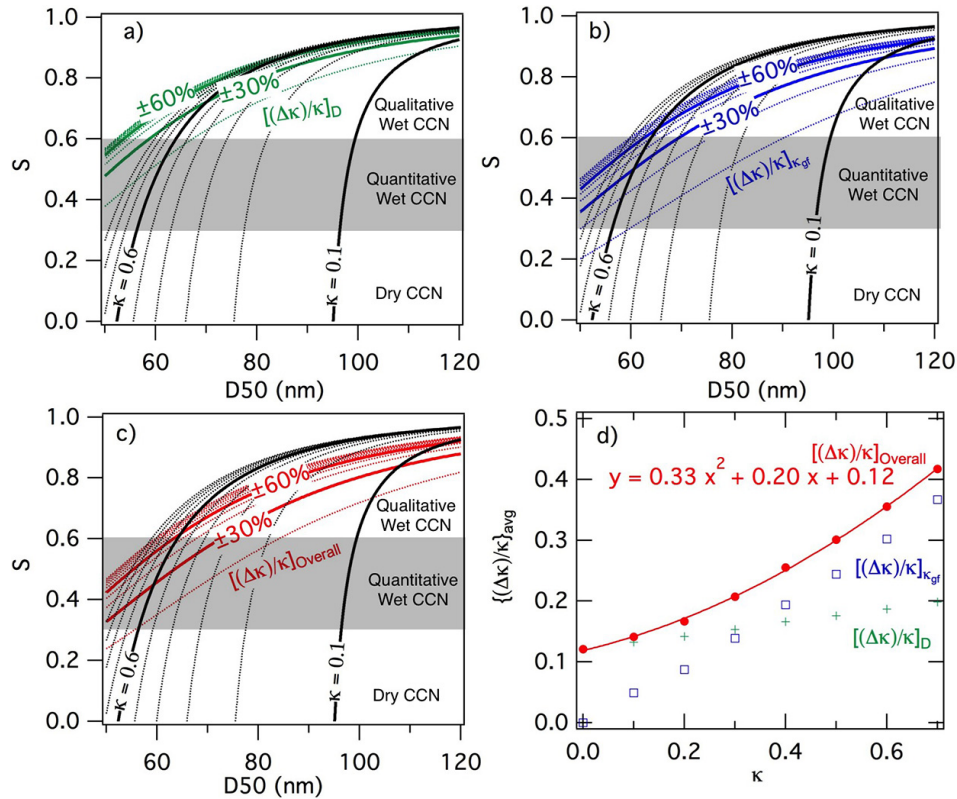
The observations for ammonium sulfate agreed reasonably well with the E-AIM prediction; the agreement in terms of D was generally within 4%. The impact of this error on the derived κ is discussed below. Efflorescence of ammonium

sulfate was observed at RH = 38%, which is slightly higher than the previously reported measurement range: $35 \pm 2\%$ ($\sim 1\,\mu m$ particles; < 1 min; Han and Martin, 1999; Martin, 2000) and 31% (75–190 nm particles; < 30 s; Smith et al., 2013). The efflorescence RH (ERH) of ammonium sulfate depends on particle size, observation time, and heterogeneous nuclei; generally, larger particle size, longer observation time, and/or the presence of heterogeneous nuclei enhance ERH (Martin, 2000; Gao et al., 2006). For particles smaller than $\sim 30\,nm$, the Kelvin effect can significantly increase ERH of ammonium sulfate (Gao et al., 2006). Considering the particle size at the point of efflorescence (83 nm) and the residence time between the humidifier and the DMA ($\sim 6\,s$), the ERH is expected to be $\sim 31\%$ (Gao et al., 2006). Therefore, the discrepancy is likely to be due to a minuscule amount of insoluble impurity in particles that can serve as a nucleus for crystallization (Martin, 2000), which would not affect the volume-based κ observation significantly. Note that the particles were in a metastable solution state, since they passed through a humidifier (at $S \sim 1.0$) prior to size selection.

Figure 4 suggests that there are two kinds of uncertainties in the Wet CCN method: (1) experimental uncertainty (the gap between the measurement and the E-AIM model, shown as the shaded area), and (2) the impact of assuming $\kappa_{gf} = \kappa_{CCN}$ (differences would result in the deviation from the κ isolines). The impact of the experimental error (< 4% in D) on κ determination depends on S and D; as can be seen in Fig. 4, the κ isolines are widely separated in the lower-right region of the contour (lower κ and lower S). To visualize

Figure 5. Error analysis of the Wet CCN method. **(a)** Impact of experimental error (represented as $\pm 4\%$ change in D) on κ, shown as isolines of the fractional error in derived κ in increments of $\pm 10\%$. **(b)** Impact of uncertainty in κ_{gf}/κ_{CCN} (represented as $\pm 50\%$ change, $\kappa_{gf}/\kappa_{CCN} = 0.5 \sim 1.5$), **(c)** overall error, combining a and b, **(d)** overall errors averaged between $S = 0.3 \sim 0.6$ as a function of κ.

the sensitivity of the κ measurement in the S vs. D space, the relative error $(\Delta \kappa / \kappa)$ that would result from the experimental error was computed by solving Eq. (11) for κ,

$$\kappa = \frac{\frac{4A^3}{27\ln^2(S_c)}}{D^3 - \frac{4A^3}{27\ln^2(S_c)}\left(\frac{S/\exp(\frac{A}{D})}{1-S/\exp(\frac{A}{D})}\right)}, \qquad (12)$$

and calculating bounds of κ for $\pm 4\%$ variations in $D([\kappa]_{+D}$ and $[\kappa]_{-D}$):

$$[\kappa]_{\pm D} =$$

$$\frac{\frac{4A^3}{27\ln^2(S_c)}}{[D \cdot (1 \pm 0.04)]^3 - \frac{4A^3}{27\ln^2(S_c)}\left(\frac{S/\exp(\frac{A}{D\cdot(1\pm0.04)})}{1-S/\exp(\frac{A}{D\cdot(1\pm0.04)})}\right)}. \qquad (13)$$

Then the relative error is estimated as follows:

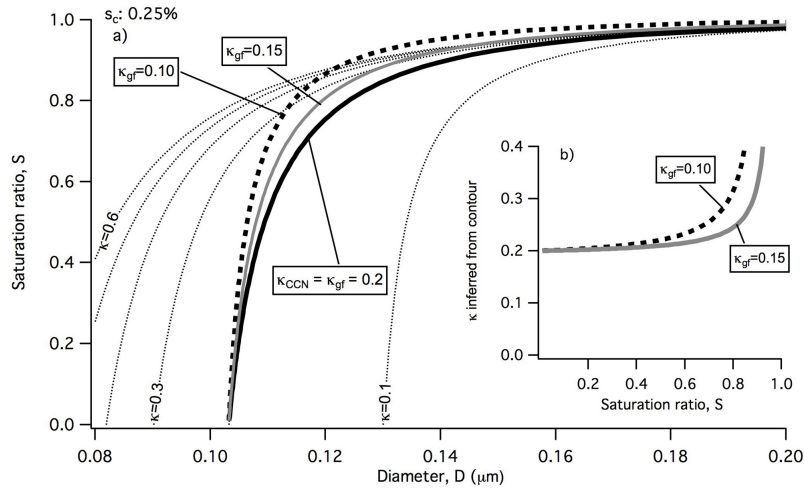$$\left[\frac{\Delta \kappa}{\kappa}\right]_D = \pm \frac{\left|[\kappa]_{+D} - [\kappa]_{-D}\right|}{2\kappa}. \qquad (14)$$

The resulting estimates are shown in Fig. 5a as isolines for every $\pm 10\%$ increment in error, with the isolines for $\pm 30\%$ and $\pm 60\%$ shown as heavier lines. The calculations assumed

$s_c = 0.40\%$, but since the experimental error is expressed as a normalized quantity $(\Delta D/D = \pm 4\%)$, the relative location of the error isolines $(|\Delta\kappa/\kappa|_D)$ to κ isolines does not depend significantly on the s_c setting. Figure 5a shows that the κ measurement in S vs. D space loses its sensitivity at high S (e.g., $\kappa = 0.6$ becomes $\pm 30\%$ uncertain at $S \sim 0.7$).

In addition, the assumption that $\kappa_{CCN} = \kappa_{gf}$ used to derive Eqs. (8) and (11) can have a significant impact on the determination of κ. For example, Fig. 6 shows trajectories for three different $\kappa_{CCN} : \kappa_{gf}$ scenarios. Note that when $\kappa_{gf} < \kappa_{CCN}$, the κ values inferred from the contours (calculated by Eqs. 8 or 11) are (erroneously) higher than κ_{CCN} (Fig. 6b). Again, the impact of the $\kappa_{CCN} : \kappa_{gf}$ ratio depends on S and D (better sensitivity at low S, low κ, and large D). Furthermore, κ_{gf} may change as a function of S, due to factors such as solubility limitations and solution non-ideality (Petters et al., 2009c).

In order to evaluate the complex effects of κ_{gf}, we estimated the impact of κ_{gf}/κ_{CCN} with $\pm 50\%$ variability (ranging from 0.5 to 1.5), which encompasses the majority, if not all, of the range of agreements between κ_{gf} and κ_{CCN} observed in previous studies (Petters et al., 2009a; Jurányi et al., 2013; Whitehead et al., 2014). The impact of $\pm 50\%$

Figure 6. Illustration of the impact of $\kappa_{gf} : \kappa_{CCN}$ on the Wet CCN analysis (s_c: 0.25 %): **(a)** predicted trajectories for different κ_{gf}; **(b)** inferred κ values for different κ_{gf}. The impact of $\kappa_{gf} : \kappa_{CCN}$ on the observed κ value increases at higher S (above ~ 0.6).

variability in κ_{gf} can be described by modifying Eq. (11):

$$D = \left(\frac{4A^3}{27\kappa \ln^2(S_c)} \right)^{1/3}$$

$$\left(1 + [\kappa \cdot (1 \pm 0.5)] \frac{S/\exp(\frac{A}{D})}{1 - S/\exp(\frac{A}{D})} \right)^{1/3}. \quad (15)$$

Solving Eq. (15) for κ, the following equation can be derived to evaluate the bounds of κ for ± 50 % variations in κ_{gf} ($[\kappa]_{+\kappa gf}$ and $[\kappa]_{-\kappa gf}$):

$$[\kappa]_{\pm \kappa gf} = \frac{\frac{4A^3}{27\ln^2(S_c)}}{D^3 - \frac{4A^3}{27\ln^2(S_c)}(1 \pm 0.5)\left(\frac{S/\exp(\frac{A}{D})}{1 - S/\exp(\frac{A}{D})} \right)}. \quad (16)$$

The relative error is estimated as follows:

$$\left[\frac{\Delta\kappa}{\kappa} \right]_{\kappa gf} = \pm \frac{\left| [\kappa]_{+\kappa gf} - [\kappa]_{-\kappa gf} \right|}{2\kappa}. \quad (17)$$
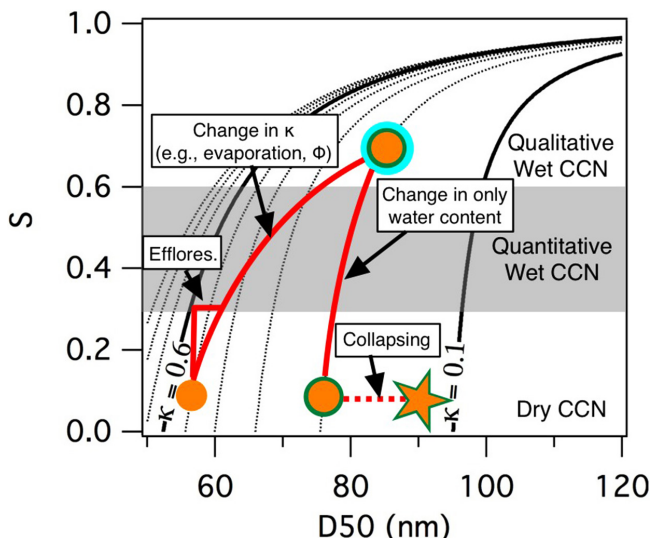
The resulting errors evaluated in the S vs. D space are shown in Fig. 5b. The overall trends of the error contours in Fig. 5a and b are similar, but the variations in κ_{gf}/κ_{CCN} introduced larger errors at a given S. Considering the overall error as the product of two independent random errors ($\Delta D/D = \pm 4$ %; $\Delta(\kappa_{gf}/\kappa_{CCN}) = \pm 50$ %), the overall error is calculated as follows (Taylor, 1997):

$$\left[\frac{\Delta\kappa}{\kappa} \right]_{Overall} = \sqrt{ \left[\frac{\Delta\kappa}{\kappa} \right]_D^2 + \left[\frac{\Delta\kappa}{\kappa} \right]_{\kappa gf}^2 }. \quad (18)$$

Using Eq. (18), the overall error contours can be calculated, as shown in Fig. 5c. Based on the results in Fig. 5c,

we recommend the quantification range over which experiments should be conducted as $S = 0.3 \sim 0.6$. Measurements at $S > 0.6$ are useful for qualitative analyses, but are not suited for quantification of κ due to the large error; $S < 0.3$ is of less interest as this range approaches the S used in conventional Dry CCN measurement, with its associated shortcomings. The average of the overall errors in this recommended range ($0.3 \leq S \leq 0.6$) for each κ isoline is shown in Fig. 5d; the experimental error ($[(\Delta\kappa)/\kappa]_D$) dominates for lower κ and the uncertainty in κ_{gf} ($[(\Delta\kappa)/\kappa]_{\kappa gf}$) dominates for higher κ, with the transition occurring around $\kappa \sim 0.3$. The overall error fitted to a quadratic equation can be used to calculate uncertainty in the Wet CCN quantification. For instance, by curve fitting ammonium sulfate data points within the quantification range (Fig. 4, excluding effloresced data points), $\kappa_{(NH4)2SO4}$ is determined to be 0.51. Using the quadratic equation in Fig. 5d, $\Delta\kappa$ is calculated to be 0.16, hence $\kappa_{(NH4)2SO4}$ is reported as 0.51 ± 0.16. Although the value is reasonable, the uncertainty is relatively large for this high κ range, which is the inherent limitation of the Wet CCN method. On the other hand, the measurement of glucose was relatively precise; the curve fit of glucose data yielded $\kappa_{glucose} = 0.17 \pm 0.03$ (Fig. 4), in good agreement with previous measurements (0.165 ± 0.033; Ruehl et al., 2010), as well as with $\kappa_{Raoult} = 0.154$ predicted for an ideal glucose solution.

The above analysis shows that the Wet CCN method, when applied to data obtained within the $S = 0.3$–0.6 range, determines κ values of typical continental aerosol ($\kappa \sim 0.3 \pm 0.1$) and marine aerosol ($\kappa \sim 0.7 \pm 0.2$) (Andreae and Rosenfeld, 2008), within $\sim \pm 20$ % and $\sim \pm 40$ %, respectively. The Wet CCN method has advantages over the conventional Dry CCN when physical/chemical properties of particles, such as shape and hydrate formation, lead to uncertainties in κ that are larger than the uncertainty range of the method; otherwise,

Figure 7. Illustration of CCN state space. Orange: hygroscopic fraction of aerosol; green: less hygroscopic fraction; blue: water.

the Dry CCN method would suffice to obtain κ estimates. The following section illustrates such applications.

3.4 Interpretation of S vs. D as "CCN state space"

The trajectories of the S vs. D relationships can be used to infer physical processes impacting the state of CCN when certain assumptions can be made, as indicated in Fig. 7. κ-Köhler curves for a set point of $s_c = 0.40\%$ in the CCN instrument are shown in Fig. 7. The shaded region in Fig. 7 represents the optimum quantification range as discussed in the error analysis section. The Dry CCN region represents particle equilibration at very low S (that is, the typical drying step to determine the volume of solute present). The endpoints of the κ isolines in this region indicate the dry critical diameter required for activation at $s_c = 0.40\%$ of a particle of composition κ, that is, the typical findings from the Dry CCN method, which uniquely relates D_{dry}, s_c, and κ. For example, a 60 nm dry particle with composition represented by $\kappa = 0.4$ would just activate under the selected s_c of 0.40 %. In the Wet CCN method applied to this same example particle composition, particles are equilibrated at various relative humidities and size-selected while wet; the (wet) $D50$ values determined for $s_c = 0.40\%$ are expected to trace out the $\kappa = 0.4$ isoline, with variability as discussed in the error analysis.

For all particles for which the Dry CCN method may be expected to yield accurate estimates of κ, the Wet CCN method outlined above – that is, identifying a representative κ for data over the range $S = 0.3 \sim 0.6$ (suggested quantification range: Fig. 5) – is expected to yield similar results for κ, if κ does not change with S. However, the Wet CCN method can provide additional information about the physical state

of the particle being probed, in addition to providing an accurate assessment of κ for particles for which the Dry CCN method fails. The locations of measurements in the S vs. $D50$ space, hereafter called Wet CCN state space, can potentially be used to infer that dry test particles are nonspherical, have collapsed when exposed to water vapor, or undergo efflorescence. As shown in Fig. 7, collapse of a nonspherical particle into a more spherical shape would result in a gap between D_{dry} that the Dry CCN method would "erroneously" provide and D extrapolated down to a dry condition ($S \sim 0$) along a κ isoline with the "correct" representative κ value obtained from the observations at high equilibration S. More specifically, collapse of particles can occur within the Nafion humidifier, where particles are exposed to $S \sim 1.0$; efflorescence can occur immediately after the humidifier when sample temperature increases from the dew point (set by the humidifier) to room temperature.

In a case where nonspherical particles collapse to become spherical particles after humidification, the dynamic shape factor of nonspherical CCN, χ (Rose et al., 2008), can be estimated as follows:

$$\chi = \frac{D_{dry\_DryCCN}}{D_{dry\_WetCCN}} \frac{C(D_{dry\_WetCCN})}{C(D_{dry\_DryCCN})}, \qquad (19)$$

where D_{dry_DryCCN} is D_{dry} measured by the conventional Dry CCN method (e.g., ~ 90 nm in Fig. 7), D_{dry_WetCCN} is the end point of a κ isoline (determined by the Wet CCN method) in the dry region (e.g., ~ 75 nm in Fig. 7), and $C(D_{dry\_DryCCN})$ and $C(D_{dry\_WetCCN})$ are the slip correction factors for the respective diameters D_{dry_DryCCN} and D_{dry_WetCCN}. $C(D)$ can be approximated as follows (Allen and Raabe, 1985):

$$C(D) = 1 + \frac{2\lambda}{D}\left[1.142 + 0.558\exp\left(-\frac{0.999D}{2\lambda}\right)\right], \qquad (20)$$

where λ is the mean free path of air molecules ($\lambda = 65.1$ nm at $T = 298$ K and 1 atm) (Seinfeld and Pandis, 2006). The major uncertainty of Eq. (19) is the estimation of D_{dry_WetCCN} by extrapolation of Wet CCN measurements ($0.3 < S < 0.6$) to dry conditions (S–0); thus the uncertainty is governed by the overall uncertainty of the Wet CCN method (Fig. 5d). Since $\kappa \propto D_{dry}^{-3}$ at fixed S_c (Eq. 7), the uncertainty of extrapolated D_{dry} is $\sim 1/3$ of the uncertainty of κ (Taylor, 1997; Kreidenweis et al., 2009):

$$\frac{\Delta\kappa}{\kappa} \approx -3\frac{\Delta D_{dry}}{D_{dry}}. \qquad (21)$$

Therefore, although the nonlinearity of $C(D)$ hinders direct comparison, the uncertainty in χ determined by Eq. (19) is approximately 1/3 of the overall uncertainty of κ determined by the Wet CCN method (Fig. 5d).

Efflorescence would be manifested as a gap in the observable $D50$ of metastable state particles and an unchanging $D50$ in the CCN instrument, regardless of the choice of

initial equilibration S; again, the "correct" representative κ value is expected at high equilibration S. This behavior is properly labeled efflorescence since atomized particles are passed through the Nafion tube at $S \sim 1.0$ and remain in a metastable state until S drops below the efflorescence S, which is the feature of this method enabling the use of spherical, deliquesced particles.

Phase partitioning, i.e., evaporation or co-condensation, of semivolatile compounds (Topping and McFiggans, 2012; Topping et al., 2013) may also occur during hygroscopic growth and cloud droplet activation. For instance, a number of studies reported evaporation (as a result of chemical decomposition) of ammonium nitrate (Mikhailov et al., 2004; Svenningsson et al., 2006; Gysel et al., 2007; Wu et al., 2013) and organic acids (Prenni et al., 2003) during H-TDMA measurements. Semivolatile compounds may also evaporate inside the CCNC (Asa-Awuku et al., 2009; Romakkaniemi et al., 2014).

The impact of phase partitioning on the Wet CCN method should depend on two major factors: (1) where the shift in partitioning occurs, particularly whether upstream or downstream of the DMA, and (2) whether evaporation is reversible, i.e., whether evaporated semivolatiles come back into the particle phase upon re-humidification within the CCNC. For example, the "Change in κ" scenario in Fig. 7 illustrates the case where evaporation of semivolatile water-soluble compounds (in green) irreversibly occurs upstream of the DMA (e.g., during humidification in a Nafion tube), which may be possible if the partitioning of semivolatile compounds is mediated by water (Topping and McFiggans, 2012). In this case, $D50$ will deviate from a κ isoline because of the change in particle composition.

However, if the evaporation occured after DMA selection (e.g., within the CCNC), the observed κ would be biased low by overestimating V_s, since it is based on the original size-selected particle before evaporation occurred. This scenario may be encountered in the Dry CCN method since some aerosol components are semivolatile, resulting in potential biases in the Dry CCN method. Currently the relative importance of evaporation upstream or downstream of the DMA is unknown. Combining the Wet CCN method and an evaporation model that predicts particle changes in the CCNC (Romakkaniemi et al., 2014) may shed light on the issue. Applying the interpretations suggested by Fig. 7 to observed deviations from κ isolines can offer insights into the nature of the measured aerosol, but caution must be taken since several different processes can cause such deviations (e.g., evaporation, change in Φ, solubility limit), with significant error (Fig. 5d: e.g., $\sim \pm 20\%$ for $\kappa \sim 0.3$).

In summary, the proposed most appropriate applications of the Wet CCN state space (Fig. 7) are as follows:

1. In the simplest case, where particles can be assumed to be spherical, nonvolatile, and $\kappa_{gf}/\kappa_{CCN} = 0.5 \si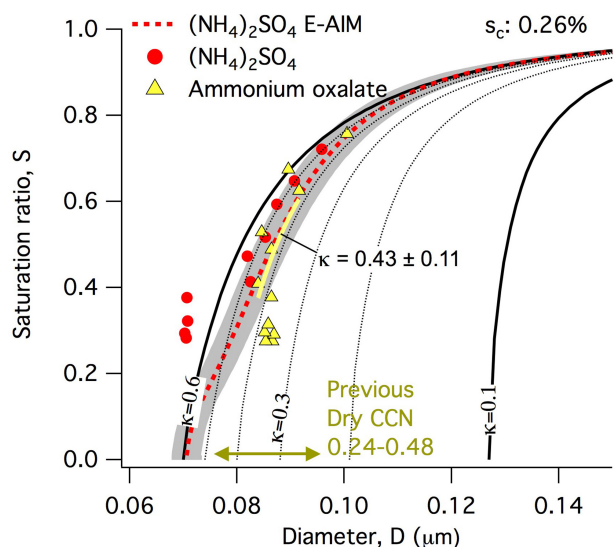m 1.5$, κ can be inferred from measurements made within $S =$ 0.3 $\sim$ 0.6, with the estimated overall error as shown in Fig. 5d. Although the Dry CCN method is sufficient to acquire κ_{CCN} for samples meeting these assumed criteria, the Wet CCN method is an effective way to evaluate the validity of the assumptions needed to apply the Dry CCN method.

2. When dry particles are assumed to be nonvolatile and nonspherical, and wet particles are spherical, the Wet CCN method provides an accurate estimate of κ without being affected by particle shape, and thus an improvement over the Dry CCN method. Furthermore, if a Dry CCN measurement and a Wet CCN measurement (e.g., differences in derived κ) are significantly different (based on the uncertainty, Fig. 5d), the ratio can be used to infer the dynamic shape factor based on the ratio of the mobility diameter of a nonspherical particle to its volume-equivalent diameter, as well as corresponding slip correction factors (Rose et al., 2008).

3. When κ can be reasonably estimated from particle composition, then the phase partitioning process can be evaluated with Wet CCN experiments since κ and V_s (impacted by evaporation) are coupled parameters (Eq. 4). The challenge is to evaluate the partitioning at different locations (e.g., before/after the DMA), which may require additional assumptions or modeling (e.g., Romakkaniemi et al., 2014).

4 Results and discussions

4.1 Ammonium oxalate

The Wet CCN approach was applied to ammonium oxalate monohydrate particles as an example system of nonspherical crystals (Hori et al., 2003), for which the Dry CCN method will overestimate solute volume and underestimate κ. Previous studies reported a large range of $\kappa_{CCN} = 0.24$–0.48 for ammonium oxalate monohydrate (Hori et al., 2003; Petters et al., 2009b). The results of the Wet CCN measurement of ammonium oxalate, along with ammonium sulfate data, are shown in Fig. 8. κ of ammonium oxalate was observed to be 0.43 ± 0.11, which is on the higher end of the previous measurement range. For $S > 0.4$, the trends of ammonium sulfate and ammonium oxalate were indistinguishable within the experimental uncertainty. The deviation of the trends for dry conditions ($S \sim 0.3$) suggests that ammonium oxalate may be in a nonspherical crystalline state as reported by Hori et al. (2003). However, unambiguous determination of particle shape would require additional measurements. For comparison, from Eq. (5) and the molar volume of ammonium oxalate ($94.7 \text{ cm}^3 \text{ mole}^{-1}$) (Haynes, 2013), κ_{Raoult} of ammonium oxalate is estimated to be 0.57 (ν is assumed to be 3), suggesting that some previous measurements of ammonium oxalate κ have likely underestimated its value.
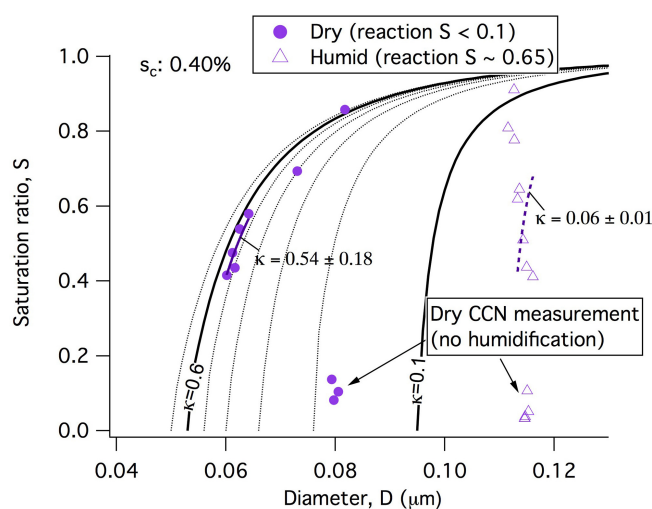
Figure 8. Data obtained using the Wet CCN method for ammonium oxalate and ammonium sulfate.

Figure 9. Wet CCN measurements for iodine oxide particles produced by CH_2I_2 photolysis and oxidation by O_3. Aerosol generation experiments were carried out at two humidity conditions as shown.

A previous study employing the electrodynamic balance (EDB) technique (Peng and Chan, 2001) observed efflorescence of ammonium oxalate at $a_w \sim 0.5$. The observed trend in Fig. 8 is consistent with the possible efflorescence at $S \sim 0.5$; the lack of a clear abrupt change in particle size may be because size reduction by loss of water was counteracted by changes in particle shape. Again, additional measurements of particle shape would be needed for verification. This measurement demonstrates the effectiveness of the Wet CCN method to determine the solute volume and κ of nonspherical water-soluble crystals, and regardless of their hydration states.

4.2   Iodine oxide particles

Results of representative IOP generation experiments carried out in dry (reactor $S < 0.1$) and humid conditions (reactor $S \sim 0.65$) are shown in the Wet CCN state space in Fig. 9. For the dry generated particles, the $D50$ of dry particles (~ 80 nm at $S \sim 0.1$) clearly deviated from the trend at higher equilibration S, suggesting nonsphericity and collapse when wetted; the κ of collapsed IOP was observed to be in the range of 0.54 ± 0.18. Assuming I_2O_5 (molar volume 67.0 cm^3 mole^{-1}) (Haynes, 2013) hydrating to become two HIO_3, as the first order approximation, κ_{Raoult} in an ideal solution is calculated to be 0.51 (further dissociation of HIO_3 would enhance κ_{Raoult}).

The comparison of the Dry CCN and the Wet CCN measurements provides semi-quantitative insights on particle shape and density. The ratio of the κ measured by the Dry CCN ($\kappa = 0.17$) to the Wet CCN κ (0.5–0.6) suggests that the nonspherical dry particle volume was observed to be 2.9–3.5 times larger than the equivalent volume of spherical particles (note that κ and V_s are coupled parameters, Eq. 5).

Assuming material density of 5 g cm^{-3} (cf., I_2O_5 density: 4.98 g cm^{-3}; CRC handbook) (Haynes, 2013), the effective density of nonspherical particles would be $1.4 \sim 1.7$ g cm^{-3}. Jimenez et al. (2003) estimated the effective density of nonspherical IOP to be 0.86–1.22 g cm^{-3} by comparing the (vacuum) aerodynamic diameter and the mobility diameter. The difference in the effective densities indicates that IOP produced in this study was more compact than that in their study; a possible reason for the discrepancy of particle shape is the different gas and particle concentration levels (Jimenez et al., $CH_2I_2 < 50$ ppb; this study: $CH_2I_2 \sim 500$ ppb), but a definitive explanation requires further experimental evaluation.

On the other hand, particle generation reactions carried out under humid conditions resulted in low hygroscopicity particles, with $\kappa = 0.06 \pm 0.01$. The unchanging $D50$ with respect to S suggests that efflorescence S is > 0.92 (highest value observed in the experiment). Again, note that deliquescence is not observed in the CCN state space since particles pass through a humidifier at $S \sim 1.0$. The derived κ value may be underestimated if particles are nonspherical (as in the dry-condition experiment). It is clear that chemical compositions of IOP in the two experiments (dry and humid) are significantly different, resulting in dramatically different efflorescence S.

A similar observation regarding a strong dependence of hygroscopicity on relative humidity during the particle generation reactions was made by Jimenez et al. (2003) semi-quantitatively using an H-TDMA. In their humid experiments (reactor $S \sim 0.65$), the hygroscopic growth factor (final diameter/initial diameter) remained nearly 1, that is, little to no water uptake was observed; by contrast, in the dry experiment (reactor $S < 0.02$), IOP started collapsing when exposed to S beyond 0.23, and then the particle regained its
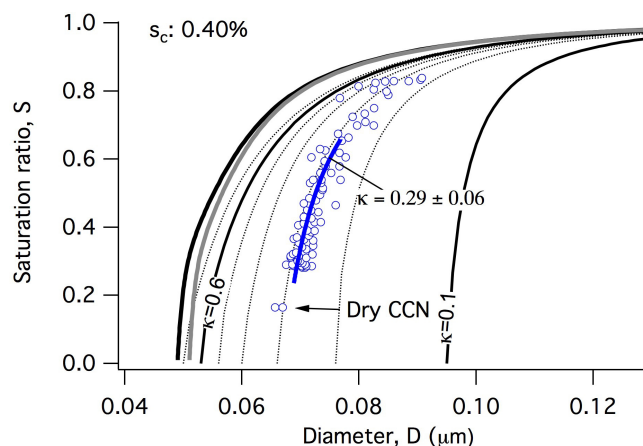
initial size at $S \sim 0.85$ by hygroscopic growth of the collapsed particles, indicative of high κ (Fig. 7 in Jimenez et al., 2003). The low hygroscopicity particles (generated in humid experiments) were inferred to be I_2O_4 based on its lack of water solubility (prolonged treatment in excess of water decomposes I_2O_4 into I_2 and HIO_3) (Daehlie and Kjekshus, 1964), instead of highly soluble I_2O_5 (263 g of I_2O_5 per 100 g of H_2O; Kumar et al., 2010); note that this solubility is sufficient for CCN activation, i.e., deliquescence S is less than the critical saturation ratio and cloud droplet activation is determined by κ_{CCN} (Petters and Kreidenweis, 2008).

However, a later study investigated the elemental composition of IOP generated photochemically by I_2 and O_3 and suggested that the main constituent is likely to be I_2O_5 (Saunders and Plane, 2005). Hence, the apparent contradiction has been a matter of debate (Murray et al., 2012; Saiz-Lopez et al., 2012). To address the contradiction, Murray et al. (2012) investigated the hygroscopicity of iodic acid (HIO_3), a hydrated form of I_2O_5, using EDB. They observed surprisingly low hygroscopicity ($\kappa = 0.024$) for this highly soluble inorganic compound. The reason for the weak hygroscopic growth was unclear, but one hypothesis was formation of polymeric structures that lead to strongly nonideal behavior (Murray et al., 2012).

The reason for the discrepancy of particle hygroscopicity depending on "reaction humidity" (not to be confused with "measurement humidity" in the Wet CCN method), remains unclear. κ of the ideal solution of I_2O_5 would be as high as typical inorganic salts (as discussed above); this appears to be consistent with the dry reaction experiments in this study and the experiments reported by Jimenez et al. (2003); in contrast, κ of humid reaction experiments was observed to be much lower ($\kappa = 0.06 \pm 0.01$), which was consistent with humid reaction experiments in Jimenez et al. (2003), as well as with EDB analysis of HIO_3 by Murray et al. (2012) ($\kappa = 0.024$). Although further studies are needed to resolve the dichotomy, considering the significance of IOP in the marine and coastal environment (Saiz-Lopez et al., 2012), the humid reaction experiments yielding low κ IOP are expected to be more atmospherically relevant.

4.3 Ammonium nitrate

Evaporation of volatile compounds after DMA sizing (inside a CCNC) would result in overestimation of $D50$ determined by the Dry CCN method (Asa-Awuku et al., 2009; Romakkaniemi et al., 2014). Recently, Romakkaniemi et al. (2014) modeled evaporation and co-condensation inside the DMT CCNC (the same instrument as used in this study), using a computational fluid dynamics model. In a test case for ammonium nitrate particles, simulation results showed that evaporation of ammonium nitrate led to a reduction in effective dry diameter by 10 to 15 nm for supersaturations between 0.1 % and 0.7 % (Romakkaniemi et al., 2014).

Figure 10. Wet CCN measurements for ammonium nitrate particles. Theoretical prediction for NH_4NO_3 is made by assuming $\kappa = 0.73$ (Kreidenweis et al., 2009) at the Dry CCN condition (x-intercept, $S = 0$) and calculating the subsequent hygroscopic growth ($S > 0$) by E-AIM (Black solid line: assuming volume additivity, Gray solid line: corresponding to wet volume output by E-AIM).

As the first step to evaluate the impact of evaporation on the Wet CCN method, ammonium nitrate was tested experimentally (Fig. 10). The theoretical prediction was made by using $\kappa = 0.73$ (Kreidenweis et al., 2009) for the x-intercept (D_{dry}) and calculating hygroscopic growth ($S > 0$) using E-AIM (Wexler and Clegg, 2002) with and without the assumption of volume additivity (black and gray solid lines). The observed $D50$ trend was significantly larger than the E-AIM prediction, with a difference of approximately 15 nm at $s_c = 0.4 \%$. The extent of the gap is consistent with Romakkaniemi et al. (2014) (at the same s_c). In contrast, Svenningsson et al. (2006) did not observe significant evaporation of NH_4NO_3; Petters and Kreidenweis (2007) analyzed the data in terms of κ and acquired $\kappa = 0.67$. The discrepancy may be due to the different operating temperatures of CC-NCs. Svenningsson et al. (2006) used a thermal gradient diffusion cloud condensation nucleus spectrometer (CCN spectrometer, University of Wyoming, CCNC-100B) that generates supersaturation by cooling the bottom plate thermoelectrically (Snider and Brenguier, 2000); on the other hand, the DMT CCNC generates supersaturation by creating a positive temperature gradient (Roberts and Nenes, 2005). Asa-Awuku et al. (2009) compared the DMT CCNC and a static diffusion CCN counter that operates below room temperature and concluded that secondary organic aerosol generated by β-caryophyllene ozonolysis evaporated significantly in the DMT CCNC due to the higher operating temperature.

The observation suggests that the presence of water in the Wet CCN method did not suppress evaporation (as a result of chemical decomposition) of NH_4NO_3 significantly. Although higher relative humidity lowers the NH_4NO_3 dissociation constant (Stelson and Seinfeld, 1982), the higher

temperature and the wall wetted by pure water in a CCNC might have enhanced the removal of particle phase NH_4NO_3 (Romakkaniemi et al., 2014). Further studies are needed for determining the upper limit of volatility for compounds for which the Wet CCN method can accurately determine κ.

5 Limitations and potential applications of the Wet CCN approach

It remains challenging to experimentally constrain individual physicochemical parameters such as surface tension, molar volume, solubility, and osmotic coefficient since they all affect the trajectory of S vs. D in different ways. Therefore, parameterization of hygroscopicity using a parameter such as κ, which folds in effects from these other variables into a single observable property, remains a practical approach. Application of the Wet CCN method to single-component particles is relatively straightforward if solutes are effectively nonvolatile and wet particles are dissolved and spherical (e.g., ammonium oxalate monohydrate). Crystal shape (which affects DMA sizing) and the presence of hydrated water in the particle volume are no longer an issue if fully deliquesced droplets can be used for characterization, as in the Wet CCN method. However, particles with a nonspherical rigid backbone may remain nonspherical even after wetting, reintroducing uncertainty in the sizing of the wet particle.

If evaporation/co-condensation of volatile compounds occurs after DMA sizing, it will lead to overestimation/underestimation in $D50$ determination, both in the Dry CCN and the Wet CCN measurements; however, the feature of the Wet CCN comes into play if the presence of water in the particle phase impacts evaporation/co-condensation. If water significantly suppresses evaporative loss of semivolatile species (Topping and McFiggans, 2012), then the Wet CCN approach allows for an experimental look at this problem. If evaporation/co-condensation occurs and results in significant changes in hygroscopicity before DMA sizing, data points in the Wet CCN state space are expected to deviate from κ isolines as described in Fig. 7. However, concentration-dependent non-ideality (Φ) (e.g., ammonium sulfate in Fig. 4) or phase separation in complex mixtures may also result in deviation from κ isolines due to the change in κ_{gf} especially at higher S ($> \sim 0.6$) (Fig. 6); therefore, again, the Wet CCN measurement needs to be limited to modest S (0.3–0.6) for quantitative analysis (Fig. 5).

Thus the major limitation of the Wet CCN technique appears to be the lack of sensitivity for high κ (e.g., $\sim \pm 40\%$ for $\kappa \sim 0.7$) and the uncertainty in identifying the cause of observed deviations from κ isolines. The potential sources of such deviations include (1) shape changes, (2) concentration-dependent non-idealities (impacting κ_{gf}, not κ_{CCN}: Fig. 6), (3) solubility limits of complex mixtures, and (4) evaporation/co-condensation. At minimum, deviation from κ isolines can be used as a flag for further investigation of physical/chemical processes involving the aqueous phase that may not be apparent, or may be overlooked, in measurements made via the conventional Dry CCN method.

6 Conclusions

This study developed the conceptual basis of the Wet CCN technique, based on simple modifications of existing conventional approaches, which we term Dry CCN methods. The Wet CCN method is the direct measurement of the subsaturated portion of κ-Köhler curves, as opposed to the Dry CCN method that constrains only the dry portion of κ-Köhler curves. In the Wet CCN method, particles are not dried before sizing, enabling a series of applications to systems where dry particle characterization is difficult due to complex particle shapes or solute compositions (e.g., hydrate formation). The Wet CCN approach was evaluated using ammonium sulfate, glucose, and nonspherical ammonium oxalate monohydrate particles, and was shown to produce estimates of κ consistent with, or improved from, those previously reported in the literature. Further, the Wet CCN approach was applied to iodine oxide particles, which are nonspherical and have unknown chemical composition. Different measured hygroscopicities of IOP when they are formed in dry vs. humid reaction conditions were consistent with observations in a previous study (Jimenez et al., 2003). Ammonium nitrate was observed to evaporate significantly even with the Wet CCN method. Care must be taken in identifying the cause of deviations of measurements from κ isolines in the CCN state space, as particle shape effect, concentration-dependent solution non-idealities, solubility limitations, and evaporation/co-condensation of volatile species can all result in such deviations and may be difficult to separate observationally.

Edited by: P. Herckes

References

Albrecht, B. A.: Aerosols, Cloud Microphysics, and Fractional Cloudiness, Science, 245, 1227–1230, 1989.

Alfarra, M. R., Good, N., Wyche, K. P., Hamilton, J. F., Monks, P. S., Lewis, A. C., and McFiggans, G.: Water uptake is independent of the inferred composition of secondary aerosols derived from multiple biogenic VOCs, Atmos. Chem. Phys., 13, 11769–11789, doi:10.5194/acp-13-11769-2013, 2013.

Allen, M. D. and Raabe, O. G.: Slip correction measurements of spherical solid aerosol particles in an improved millikan apparatus, Aerosol Sci. Technol., 4, 269–286, 1985.

Andreae, M. O. and Rosenfeld, D.: Aerosol–cloud–precipitation interactions, Part 1. The nature and sources of cloud-active aerosols, Earth-Sci. Rev., 89, 13–41, 2008.

Asa-Awuku, A., Engelhart, G. J., Lee, B. H., Pandis, S. N., and Nenes, A.: Relating CCN activity, volatility, and droplet growth kinetics of β-caryophyllene secondary organic aerosol, Atmos. Chem. Phys., 9, 795–812, doi:10.5194/acp-9-795-2009, 2009.

Blando, J. D. and Turpin, B. J.: Secondary organic aerosol formation in cloud and fog droplets: a literature evaluation of plausibility, Atmos. Environ., 34, 1623–1632, 2000.

Carrico, C. M., Petters, M. D., Kreidenweis, S. M., Collett Jr., J. L., Engling, G., and Malm, W. C.: Aerosol hygroscopicity and cloud droplet activation of extracts of filters from biomass burning experiments, J. Geophys. Res., 113, D08206, doi:10.01029/02007JD009274, 2008.

Christensen, S. I. and Petters, M. D.: The Role of Temperature in Cloud Droplet Activation, J. Phys. Chem. A, 116, 9706–9717, 2012.

Daehlie, G. and Kjekshus, A.: Iodine Oxides Part I. On I2O3.SO3, I2O3.4SO3.H2O, I2O3.SeO3 and I2O4, Acta Chemica Scandinavica, 18, 144–156, 1964.

Duplissy, J., Gysel, M., Alfarra, M. R., Dommen, J., Metzger, A., Prevot, A. S. H., Weingartner, E., Laaksonen, A., Raatikainen, T., Good, N., Turner, S. F., McFiggans, G., and Baltensperger, U.: Cloud forming potential of secondary organic aerosol under near atmospheric conditions, Geophys. Res. Lett., 35, L03818, doi:10.1029/2007GL031075, 2008.

Ervens, B., Turpin, B. J., and Weber, R. J.: Secondary organic aerosol formation in cloud droplets and aqueous particles (aqSOA): a review of laboratory, field and model studies, Atmos. Chem. Phys., 11, 11069–11102, doi:10.5194/acp-11-11069-2011, 2011.

Fitzgerald, J. W., Hoppel, W. A., and Vietti, M. A.: The Size and Scattering Coefficient of Urban Aerosol Particles at Washington, DC as a Function of Relative Humidity, J. Atmos. Sci., 39, 1838–1852, 1982.

Gao, Y., Chen, S. B., and Yu, L. E.: Efflorescence Relative Humidity for Ammonium Sulfate Particles, J. Phys. Chem. A, 110, 7602–7608, 2006.

Graedel, T. E., and Weschler, C. J.: Chemistry within aqueous atmospheric aerosols and raindrops, Reviews of Geophysics, 19, 505-539, 1981.

Gysel, M., Crosier, J., Topping, D. O., Whitehead, J. D., Bower, K. N., Cubison, M. J., Williams, P. I., Flynn, M. J., McFiggans, G. B., and Coe, H.: Closure study between chemical composition and hygroscopic growth of aerosol particles during TORCH2, Atmos. Chem. Phys., 7, 6131–6144, doi:10.5194/acp-7-6131-2007, 2007.

Hallquist, M., Wenger, J. C., Baltensperger, U., Rudich, Y., Simpson, D., Claeys, M., Dommen, J., Donahue, N. M., George, C., Goldstein, A. H., Hamilton, J. F., Herrmann, H., Hoffmann, T., Iinuma, Y., Jang, M., Jenkin, M. E., Jimenez, J. L., Kiendler-Scharr, A., Maenhaut, W., McFiggans, G., Mentel, Th. F., Monod, A., Prévôt, A. S. H., Seinfeld, J. H., Surratt, J. D., Szmigielski, R., and Wildt, J.: The formation, properties and impact of secondary organic aerosol: current and emerging issues, Atmos. Chem. Phys., 9, 51550–5236, doi:10.5194/acp-9-5155-2009, 2009.

Han, J.-H., and Martin, S. T.: Heterogeneous nucleation of the efflorescence of (NH4)2SO4 particles internally mixed with Al2O3, TiO2, and ZrO2, J. Geophys. Res. Atmos., 104, 3543–3553, 1999.

Haynes, W. M.: CRC Handbook of Chemistry and Physics, 94th Edn., CRC Press, Boca Raton, Florida, United States, 2013.

Hong, J., Häkkinen, S. A. K., Paramonov, M., Äijälä, M., Hakala, J., Nieminen, T., Mikkilä, J., Prisle, N. L., Kulmala, M., Riipinen, I., Bilde, M., Kerminen, V.-M., and Petäjä, T.: Hygroscopicity, CCN and volatility properties of submicron atmospheric aerosol in a boreal forest environment during the summer of 2010, Atmos. Chem. Phys., 14, 4733–4748, doi:10.5194/acp-14-4733-2014, 2014.

Hori, M., Ohta, S., Murao, N., and Yamagata, S.: Activation capability of water soluble organic substances as CCN, J. Aerosol Sci., 34, 419-448, 2003.

Hudson, J. G. and Da, X.: Volatility and size of cloud condensation nuclei, J. Geophys. Res. Atmos., 101, 4435–4442, 1996.

IPCC, Intergovernmental Panel on Climate Change: Climate Change 2007: The Physical Science Basis, Cambridge University Press, UK, 2007.

Jimenez, J. L., Bahreini, R., Cocker, D. R., Zhuang, H., Varutbangkul, V., Flagan, R. C., Seinfeld, J. H., O'Dowd, C. D., and Hoffman, T.: New particle formation from photooxidation of diiodomethane (CH2I2), J. Geophys. Res., 108, 4318, doi:10.1029/2002JD002452, 2003.

Jurányi, Z., Tritscher, T., Gysel, M., Laborde, M., Gomes, L., Roberts, G., Baltensperger, U., and Weingartner, E.: Hygroscopic mixing state of urban aerosol derived from size-resolved cloud condensation nuclei measurements during the MEGAPOLI campaign in Paris, Atmos. Chem. Phys., 13, 6431–6446, doi:10.5194/acp-13-6431-2013, 2013.

Kreidenweis, S. M., Koehler, K., DeMott, P. J., Prenni, A. J., Carrico, C., and Ervens, B.: Water activity and activation diameters from hygroscopicity data– Part I: Theory and application to inorganic salts, Atmos. Chem. Phys., 5, 1357–1370, doi:10.5194/acp-5-1357-2005, 2005.

Kreidenweis, S. M., Petters, M. D., and Chuang, P. Y.: Cloud Particle Precursors, Clouds in the Perturbed Climate System: Their Relationship to Energy Balance, Atmospheric Dynamics, and Precipitation, edited by: Heintzenberg, J. and Charlson, R. J., The MIT Press, Cambridge, Massachusetts, 2009.

Kumar, P., Sokolik, I. N., and Nenes, A.: Parameterization of cloud droplet formation for global and regional models: including adsorption activation from insoluble CCN, Atmos. Chem. Phys., 9, 2517–2532, doi:10.5194/acp-9-2517-2009, 2009.

Kumar, P., Sokolik, I. N., and Nenes, A.: Measurements of cloud condensation nuclei activity and droplet activation kinetics of fresh unprocessed regional dust samples and minerals, Atmos.

Chem. Phys., 11, 3527–3541, doi:10.5194/acp-11-3527-2011, 2011.

Kumar, R., Saunders, R. W., Mahajan, A. S., Plane, J. M.C., and Murray, B. J.: Physical properties of iodate solutions and the deliquescence of crystalline I2O5 and HIO3, Atmos. Chem. Phys., 10, 12251–12260, doi:10.5194/acp-10-12251-2010, 2010.

Martin, M., Tritscher, T., Jurányi, Z., Heringa, M. F., Sierau, B., Weingartner, E., Chirico, R., Gysel, M., Prévôt, A. S. H., Baltensperger, U., and Lohmann, U.: Hygroscopic properties of fresh and aged wood burning particles, J. Aerosol Sci., 56, 15–29, 2013.

Martin, S. T.: Phase transitions of aqueous atmospheric particles, Chemical Reviews, 100, 3403-3454, 2000.

Massoli, P., Lambe, A. T., Ahern, A. T., Williams, L. R., Ehn, M., Mikkilä, J., Canagaratna, M. R., Brune, W. H., Onasch, T. B., Jayne, J. T., Petäjä, T., Kulmala, M., Laaksonen, A., Kolb, C. E., Davidovits, P., and Worsnop, D. R.: Relationship between aerosol oxidation level and hygroscopic properties of laboratory generated secondary organic aerosol (SOA) particles, Geophys. Res. Lett., 37, L24801, doi:24810.21029/22010gl045258, 2010.

McFiggans, G., Coe, H., Burgess, R., Allan, J., Cubison, M., Alfarra, M. R., Saunders, R., Saiz-Lopez, A., Plane, J. M. C., Wevill, D., Carpenter, L., Rickard, A. R., and Monks, P. S.: Direct evidence for coastal iodine particles from Laminaria macroalgae – linkage to emissions of molecular iodine, Atmos. Chem. Phys., 4, 701–713, doi:10.5194/acp-4-701-2004, 2004.

McFiggans, G., Artaxo, P., Baltensperger, U., Coe, H., Facchini, M. C., Feingold, G., Fuzzi, S., Gysel, M., Laaksonen, A., Lohmann, U., Mentel, T. F., Murphy, D. M., O'Dowd, C. D., Snider, J. R., and Weingartner, E.: The effect of physical and chemical aerosol properties on warm cloud droplet activation, Atmos. Chem. Phys., 6, 2593–2649, doi:10.5194/acp-6-2593-2006, 2006.

Mikhailov, E., Vlasenko, S., Niessner, R., and Pöschl, U.: Interaction of aerosol particles composed of protein and saltswith water vapor: hygroscopic growth and microstructural rearrangement, Atmos. Chem. Phys., 4, 323–350, doi:10.5194/acp-4-323-2004, 2004.

Murray, B. J., Haddrell, A. E., Peppe, S., Davies, J. F., Reid, J. P., O'Sullivan, D., Price, H. C., Kumar, R., Saunders, R. W., Plane, J. M. C., Umo, N. S., and Wilson, T. W.: Glass formation and unusual hygroscopic growth of iodic acid solution droplets with relevance for iodine mediated particle formation in the marine boundary layer, Atmos. Chem. Phys., 12, 8575–8587, doi:10.5194/acp-12-8575-2012, 2012.

Novakov, T. and Penner, J. E.: Large contribution of organic aerosols to cloud-condensation nuclei concentrations, Nature, 365, 823–826, 1993.

Peng, C. and Chan, C. K.: The water cycles of water-soluble organic salts of atmospheric importance, Atmos. Environ., 35, 1183–1192, 2001.

Petters, M. D. and Kreidenweis, S. M.: A single parameter representation of hygroscopic growth and cloud condensation nucleus activity, Atmos. Chem. Phys., 7, 1961–1971, doi:10.5194/acp-7-1961-2007, 2007.

Petters, M. D. and Kreidenweis, S. M.: A single parameter representation of hygroscopic growth and cloud condensation nucleus activity – Part 2: Including solubility, Atmos. Chem. Phys., 8, 6273–6279, doi:10.5194/acp-8-6273-2008, 2008.

Petters, M. D., Carrico, C. M., Kreidenweis, S. M., Prenni, A. J., DeMott, P. J., Collett, J. L. Jr., and Moosm uller, H.: Cloud condensation nucleation activity of biomass burning aerosol, J. Geophys. Res., 114, D22205, doi:22210.21029/22009jd012353, 2009a.

Petters, M. D., Kreidenweis, S. M., Prenni, A. J., Sullivan, A., Carrico, C. M., Koehler, K. A., and Ziemann, P. J.: Role of molecular size in cloud droplet activation, Geophys. Res. Lett., 36, L22801, doi:10.1029/2009GL040131, 2009b.

Petters, M. D., Wex, H., Carrico, C. M., Hallbauer, E., Massling, A., McMeeking, G. R., Poulain, L., Wu, Z., Kreidenweis, S. M., and Stratmann, F.: Towards closing the gap between hygroscopic growth and activation for secondary organic aerosol – Part 2: Theoretical approaches, Atmos. Chem. Phys., 9, 3999–4009, doi:10.5194/acp-9-3999-2009, 2009c.

Petters, M. D. and Kreidenweis, S. M.: A single parameter representation of hygroscopic growth and cloud condensation nucleus activity – Part 3: Including surfactant partitioning, Atmos. Chem. Phys., 13, 1081–1091, doi:10.5194/acp-13-1081-2013, 2013.

Petters, M. D., Prenni, A. J., Kreidenweis, S. M., and DeMott, P. J.: On measuring the critical diameter of cloud condensation nuclei using mobility selected aerosol, Aerosol Sci. Technol., 41, 907–913, 2007.

Prenni, A. J., DeMott, P. J., Kreidenweis, S. M., Russell, L. M., and Ming, Y.: The effects of low molecular weight dicarboxylic acids on cloud formation, J. Phys. Chem. A, 105, 11240-11248, 2001.

Prenni, A. J., DeMott, P. J., and Kreidenweis, S. M.: Water uptake of internally mixed particles containing ammonium sulfate and dicarboxylic acids, Atmos. Environ., 37, 4243-4251, 2003.

Prenni, A. J., Petters, M. D., Kreidenweis, S. M., DeMott, P. J., and Ziemann, P. J.: Cloud droplet activation of secondary organic aerosol, J. Geophys. Res., 112, D10223, doi:10.1029/2006JD007963, 2007.

Pruppacher, H. R. and Klett, J. D.: Microphysics of Clouds and Precipitation, Kluwer Academic Publishers, Dordrecht, 1997.

Rissler, J., Vestin, A., Swietlicki, E., Fisch, G., Zhou, J., Artaxo, P., and Andreae, M. O.: Size distribution and hygroscopic properties of aerosol particles from dry-season biomass burning in Amazonia, Atmos. Chem. Phys., 6, 471–491, doi:10.5194/acp-6-471-2006, 2006.

Roberts, G. C. and Nenes, A.: A continuous-flow streamwise thermal-gradient CCN chamber for atmospheric measurements, Aerosol Sci. Technol., 39, 206-221, 2005.

Romakkaniemi, S., Jaatinen, A., Laaksonen, A., Nenes, A., and Raatikainen, T.: Ammonium nitrate evaporation and nitric acid condensation in DMT CCN counters, Atmos. Meas. Tech., 7, 1377–1384, doi:10.5194/amt-7-1377-2014, 2014.

Rose, D., Gunthe, S. S., Mikhailov, E., Frank, G. P., Dusek, U., Andreae, M. O., and Pöschl, U.: Calibration and measurement uncertainties of a continuous-flow cloud condensation nuclei counter (DMT-CCNC): CCN activation of ammonium sulfate and sodium chloride aerosol particles in theory and experiment, Atmos. Chem. Phys., 8, 1153–1179, doi:10.5194/acp-8-1153-2008, 2008.

Ruehl, C. R., Chuang, P. Y., and Nenes, A.: Aerosol hygroscopicity at high (99 to 100 %) relative humidities, Atmos. Chem. Phys., 10, 1329–1344, doi:10.5194/acp-10-1329-2010, 2010.

Ruehl, C. R., Chuang, P. Y., Nenes, A., Cappa, C. D., Kolesar, K. R., and Goldstein, A. H.: Strong evidence of surface tension reduc-

tion in microscopic aqueous droplets, Geophys. Res. Lett., 39, L23801, doi:23810.21029/22012GL053706, 2012.

Saiz-Lopez, A., Plane, J. M. C., Baker, A. R., Carpenter, L. J., von Glasow, R., Gómez Martín, J. C., McFiggans, G., and Saunders, R. W.: Atmospheric Chemistry of Iodine, Chemical Reviews, 112, 1773–1804, 2012.

Sareen, N., Schwier, A. N., Lathem, T. L., Nenes, A., and Mc-Neill, V. F.: Surfactants from the gas phase may promote cloud droplet formation, Proc. Natl. Aca. Sci., 110, 2723–2728, doi:10.1073/pnas.1204838110, 2013.

Saunders, R. W. and Plane, J. M. C.: Formation Pathways and Composition of Iodine Oxide Ultra-Fine Particles, Environ. Chem., 2, 299–303, 2005.

Seinfeld, J. H. and Pandis, S. N.: Atmospheric Chemistry and Physics: From Air Pollution to Climate Change – 2nd Edn., A Wiley-Interscience publication, New Jersey, 2006.

Smith, M. L., You, Y., Kuwata, M., Bertram, A. K., and Martin, S. T.: Phase Transitions and Phase Miscibility of Mixed Particles of Ammonium Sulfate, Toluene-Derived Secondary Organic Material, and Water, J. Phys. Chem. A, 117, 8895–8906, 2013.

Snider, J. R. and Brenguier, J.-L.: Cloud condensation nuclei and cloud droplet measurements during ACE-2, Tellus B, 52, 828–842, 2000.

Snider, J. R. and Petters, M. D.: Optical particle counter measurement of marine aerosol hygroscopic growth, Atmos. Chem. Phys., 8, 1949–1962, doi:10.5194/acp-8-1949-2008, 2008.

Snider, J. R., Petters, M. D., Wechsler, P., and Liu, P. S. K.: Supersaturation in the Wyoming CCN Instrument, J. Atmos. Ocean. Technol., 23, 1323–1339, 2006.

Sorjamaa, R. and Laaksonen, A.: The effect of H_2O adsorption on cloud drop activation of insoluble particles: a theoretical framework, Atmos. Chem. Phys., 7, 6175–6180, doi:10.5194/acp-7-6175-2007, 2007.

Stelson, A. W. and Seinfeld, J. H.: Relative humidity and temperature dependence of the ammonium nitrate dissociation constant, Atmos. Environ., 16, 983–992, 1982.

Suda, S. R. and Petters, M. D.: Accurate Determination of Aerosol Activity Coefficients at Relative Humidities up to 99 % Using the Hygroscopicity Tandem Differential Mobility Analyzer Technique, Aerosol Sci. Technol., 47, 991–1000, 2013.

Svenningsson, B., Rissler, J., Swietlicki, E., Mircea, M., Bilde, M., Facchini, M. C., Decesari, S., Fuzzi, S., Zhou, J., Mønster, J., and Rosenørn, T.: Hygroscopic growth and critical supersaturations for mixed aerosol particles of inorganic and organic compounds of atmospheric relevance, Atmos. Chem. Phys., 6, 1937–1952, doi:10.5194/acp-6-1937-2006, 2006.

Taylor, J. R.: An Introduction to Error Analysis, The Study of Uncertainties in Physical Measurements, 2nd Edn., University Science Books, Mill Valley, California, 1997.

Topping, D. O. and McFiggans, G.: Tight coupling of particle size, number and composition in atmospheric cloud droplet activation, Atmos. Chem. Phys., 12, 3253–3260, 2012, http://www.atmos-chem-phys.net/12/3253/2012/.

Topping, D. O., Connolly, P., and McFiggans, G.: Cloud droplet number enhanced by co-condensation of organic vapours, Nat. Geosci., 6, 443–446, 2013.

Twomey, S.: The Composition of Cloud Nuclei, J. Atmos. Sci., 28, 377–381, 1971.

Twomey, S.: Pollution and the planetary albedo, Atmos. Environ., 8, 1251–1256, 1974.

Wex, H., Hennig, T., Salma, I., Ocskay, R., Kiselev, A., Henning, S., Massling, A., Wiedensohler, A., and Stratmann, F.: Hygroscopic growth and measured and modeled critical super-saturations of an atmospheric HULIS sample, Geophys. Res. Lett., 34, L02818, doi:10.1029/2006GL028260, 2007.

Wex, H., Petters, M. D., Carrico, C. M., Hallbauer, E., Massling, A., McMeeking, G. R., Poulain, L., Wu, Z., Kreidenweis, S. M., and Stratmann, F.: Towards closing the gap between hygroscopic growth and activation for secondary organic aerosol: Part 1 – Evidence from measurements, Atmos. Chem. Phys., 9, 3987–3997, doi:10.5194/acp-9-3987-2009, 2009.

Wexler, A. S., and Clegg, S. L.: Atmospheric aerosol models for systems including the ions H+, NH4+, Na+, SO_4^{2-}, NO_3^-, Cl^-, Br^-, and H_2O, J. Geophys. Res. Atmos., 107, 4207, doi:10.1029/2001JD000451, 2002.

Whitehead, J. D., Irwin, M., Allan, J. D., Good, N., and McFiggans, G.: A meta-analysis of particle water uptake reconciliation studies, Atmos. Chem. Phys. Discuss., 14, 9783–9800, doi:10.5194/acpd-14-9783-2014, 2014.

Wu, Z. J., Poulain, L., Henning, S., Dieckmann, K., Birmili, W., Merkel, M., van Pinxteren, D., Spindler, G., Müller, K., Stratmann, F., Herrmann, H., and Wiedensohler, A.: Relating particle hygroscopicity and CCN activity to chemical composition during the HCCT-2010 field campaign, Atmos. Chem. Phys. Discuss., 13, 7643–7680, doi:10.5194/acpd-13-7643-2013, 2013.